9 Experimental Case No. 2

In this chapter the experimental case no. 2 introduced in section 1.4.2 is described. This experimental case concerns a vibration based inspection (VBI) of a lattice steel test mast. The ideas behind VBI have been explained in section 1.2.2. VBI is divided into four levels. In this experimental case only the use of level 1 methods will be illustrated. In other words, it will only be shown how damage can be detected on the basis of modal parameter estimates. In section 9.1, the measurement procedure and the signal processing applied prior to the system identification of the mast are explained. Section 9.2 concerns the system identification of the dynamic properties of the mast in its virgin state, i.e. before the damage is introduced. The system identification of the mast in its damaged states is described in section 9.3, whereas the actual damage detection is given in section 9.4.

9.1 Data Acquisition and Signal Processing

As explained in section 1.4.2, the mast has been equipped with 6 accelerometers. However, as also explained, one of these was unfortunately destroyed during the test because of heavy rain. This section explains how the acquisition of the measurements of the five remaining accelerometers has been performed. It will also be explained how these measurements have been processed prior to the actual system identification.

The data have been sampled at 500 Hz using a 16 bit A/D converter, as well as analog antialias filtered. After sampling the data were decimated 10 times, i.e. lowpass filtered and resampled at a 10 times lower frequency. The reason for this oversampling is that it improves the signal to noise ratio in the data, since every data point is constructed from 10 samples. Thus, the resulting sampling interval becomes T = 0.02 sec. Finally, the filtered data have been detrended and calibrated to accelerations described in the unit m/sec^2. Each measurement session lasted 160 sec, which implies that the final record length has N = 8000 points. This record length is assumed to be adequate in order to obtain an accurate system identification. In figure 9.1, the data of one of the measurement sessions are presented for all five channels.

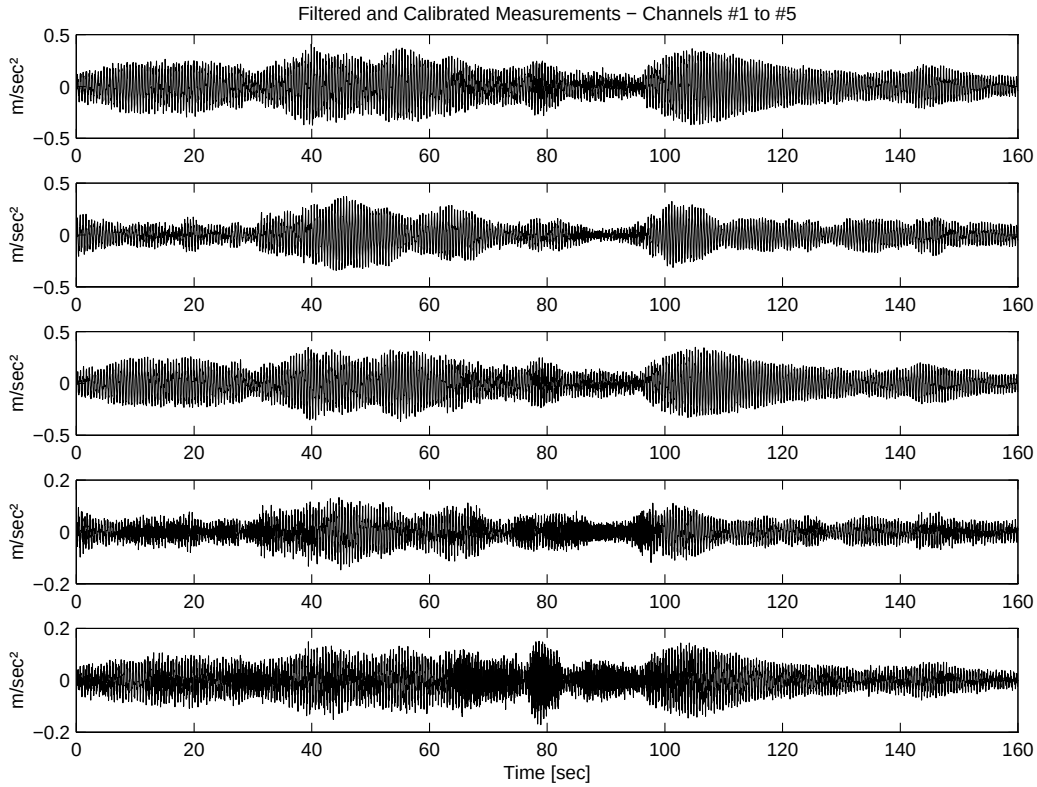

Figure 9.1: Example of the measured accelerations of the five channels.

9.2 Virgin State Analysis

In the VBI approach used in this chapter a virgin state of the structure has to be defined. In this state the dynamic properties of the structure have to be determined with as much accuracy as possible. The damage indicators of the structure identified at a later state will then be compared with the damage indicators of the virgin state. The virgin state tests of the structure were initiated at August 30, 1996 and lasted until November 4, 1996. During this period 96 measurement sessions were performed. In this section, it is described how the dynamic properties of the mast have been modelled and identified on the basis of these measurements.

9.2.1 Adequate Modelling of the Dynamic Properties

At the present state, it is not possible to determine which of the modal parameters will be sensitive to damage. However, it is assumed that some of the estimated natural eigenfrequencies or the associated damping ratios are applicable as damage indicators. Since the mode shapes are only described in a few points of the structure these will not be used in the VBI analysis as a damage indicator. This means that the system identification in principle can be performed by a univariate model structure.

However, as seen in figure 9.2 there are two closely spaced modes around 2 Hz and two closely spaced modes around 11.5 Hz.

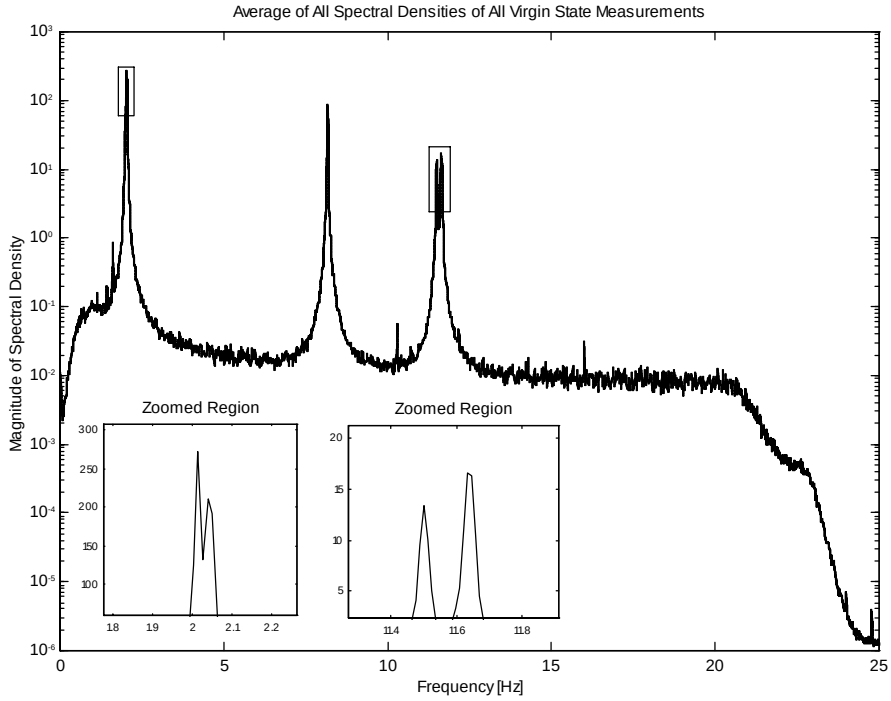

Figure 9.2: FFT-based spectral density of the response using all virgin state measurements. The auto-spectral densities and magnitudes of the cross-spectral densities of all measurement records have been averaged. All records have been normalized to unit standard deviation. The frequency resolution is 2048 between 0 and 25 Hz. The zoomed regions are the areas around the peaks at 2 Hz and 11.5 Hz.

The two modes located around 2 Hz are the first modes of bending in the two perpendicular directions, see figure 1.4. The mode located around 8 Hz is the first torsional mode of the structure, and the two modes located around 11.5 Hz are the second modes of bending. These observations are in accordance with prior research reported in Kirkegaard et al. [58], where the dynamic behaviour of the structure has been investigated through experimental studies as well as FEM analysis. Because of the closely spaced modes the most sensible choice of model structure is an ARMAV model with as many channels as possible, i.e. 5 channels. In this way information from all sensors is used. Assuming that all 5 modes are underdamped, it is necessary to use at least the ARMAV(2,1) model. However, besides modelling the five structural modes there is a significant filter characteristic present just below the Nyquist frequency as seen in figure 9.2 which also has to be modelled. This filter characteristic originates from the lowpass filter applied in the decimation procedure before the data were resampled. Further, in some of the measurements the signal-to-noise ratio is low due to a limited presence of wind.

This implies that the model structure in general must be of the ARMAV(*n*,*n*) type. The order *n* has been selected on the basis of the Akaike FPE criterion as $n = 3$. According to the results of section 3.3.1, this is also the lowest model order to use when the measurements are accelerations. This implies that the number of parameters needing to be estimated is 150. This model structure has been used in all identifications. The actual system identifications have been performed using the non-linear PEM algorithm described in chapter 5 and implemented in the routine armav.m of the STDI toolbox.

In all identifications the maximum number of iterations used in the PEM algorithm is 40. If this number is exceeded or if the RMS value of the search gradient, given by $\boldsymbol{R}_N^{-1}(\theta)\boldsymbol{F}_N(\theta)$ in definition 5.1, is less than 1.0×10^{-6} the iterations are stopped. The robustification parameter ρ defined in section 7.1.4 is set to 1.6. In figure 9.3, the adequacy of the model is illustrated by plotting the FFT-based auto-spectral densities together with the auto-spectral densities obtained from the identified ARMAV model for one of the virgin state measurement sessions.

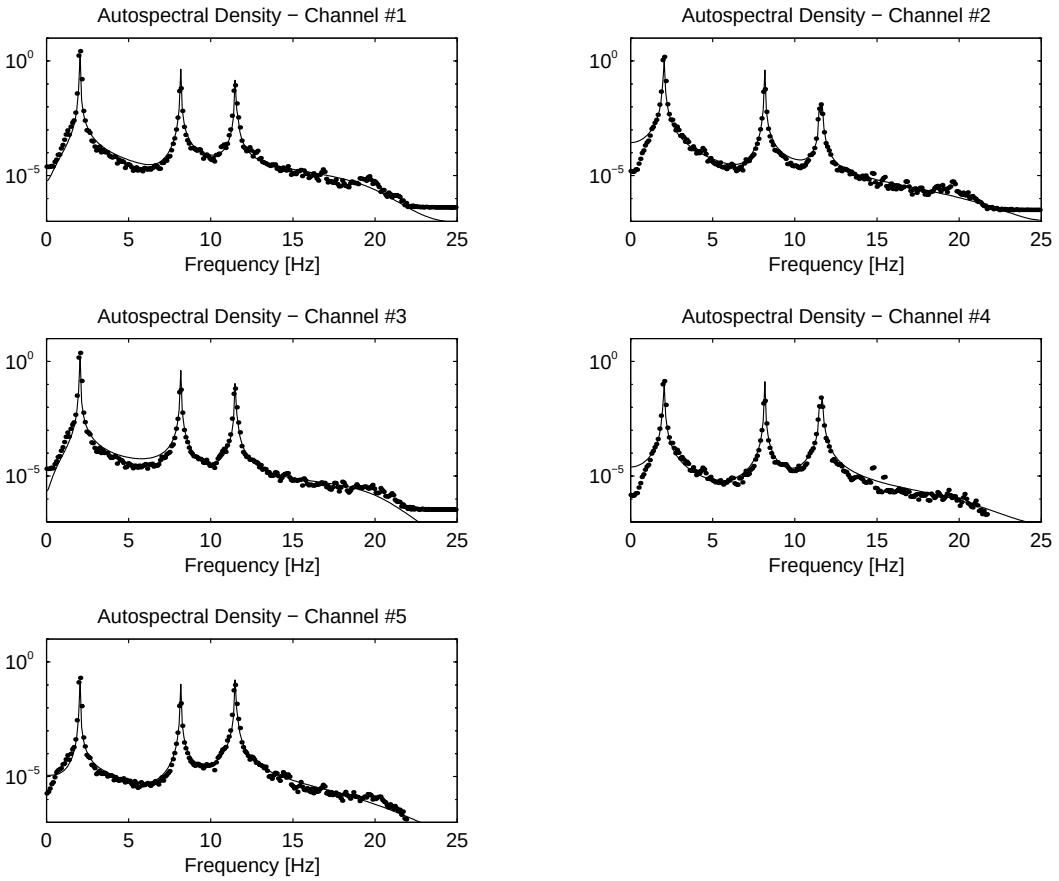

Figure 9.3: Comparison of the auto-spectral densities obtained using FFT and the estimated ARMAV(3,3) model using data from one of the virgin state measurement session.

In the damaged states of the structure, it is the intention to make use of the estimated uncertainties of the estimated modal parameters. However, as in the experimental case no. 1 the prediction errors must be Gaussian white noise for these estimates to be accurate enough. It is therefore necessary to check, whether the prediction errors are Gaussian distributed or not. This can be checked using a normal probability plot, which is illustrated in figure 9.4 for the prediction errors of an ARMAV model of one of the virgin state measurement sessions.

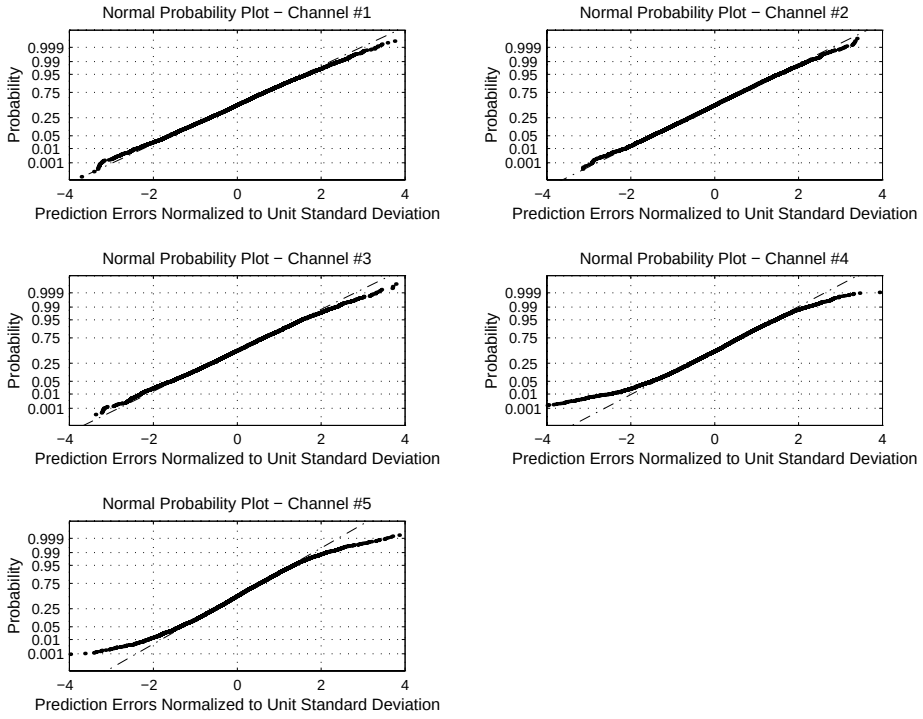

Figure 9.4: Normal probability plot of the prediction errors of an estimated ARMAV(3,3) model obtained using data from one of the virgin state measurement sessions.

In the present case the normal probability plot in figure 9.3 indicates a 95% confidence in that the prediction errors of at least the first three channels of this particular model are Gaussian distributed. Besides checking whether the prediction errors are Gaussian or not, it is also necessary to check whether the prediction errors are white noise or not. This is checked by plotting their auto-correlation functions or their spectral densities as illustrated in section 7.3.3. These two checks must be performed in all the cases where the estimated uncertainties of the modal parameters are used. If the confidence is low, the estimated uncertainties should not be used. In the following a 95% confidence is assumed adequate and any estimated models that do not have prediction errors satisfying this requirement are rejected in the damaged states analysis.

As mentioned above, 96 identifications were performed. This section describes how the structural modes have been identified from these identifications. It is the intention

to average the 96 estimates of the modal parameters and use these averaged values to describe the virgin state dynamic properties of the structure. In the same way, it is possible to describe the uncertainties of the dynamic properties of the virgin state by means of the sampled standard deviations of the modal parameter estimates.

The structural modes of the identified models have been determined by the following two stability diagrams.The stability diagram shown in figure 9.5 utilizes the MAC criterion. If the mode shape of a mode of a currently estimated model correlates with a mode shape belonging to the previously estimated model in such a sense that the MAC between these mode shapes are at least 0.95, then a circle “o” will be marked in the stability diagram. The location of this circle will be at the coordinate indicating the number of the current model and the natural eigenfrequency that corresponds to the mode shape. All identified modes of the models are marked with dots “·” and located in the same way in the diagram.

In figure 9.6, a frequency stabilization diagram is shown. Again all identified modes are marked with dots “·”. If the damping ratio of a particular mode is less than 1% the mode is marked with a circle “o”. If the natural eigenfrequencies of a mode of the current and previous models have an absolute and maximum deviation of 5%, then this mode is marked with a “+”. The modes that originate from the structural system will be underdamped. This implies that their damping ratios will be small, which can be verified by the spectral density plot in figure 9.2. Therefore, it makes sense to assume that the damping ratios of the identified structural modes are less that 1%. The modes of the noise will typically have a broad-banded nature, i.e. be more heavily damped. The natural eigenfrequencies of these modes will typically deviate from model to model, since the noise properties of the measurement records are never the same. Further, the “mode shapes” of these modes will typically deviate from model to model. This is why the MAC criterion is an efficient way to locate structural modes. See also section 6.4 for further details on identification of structural modes.

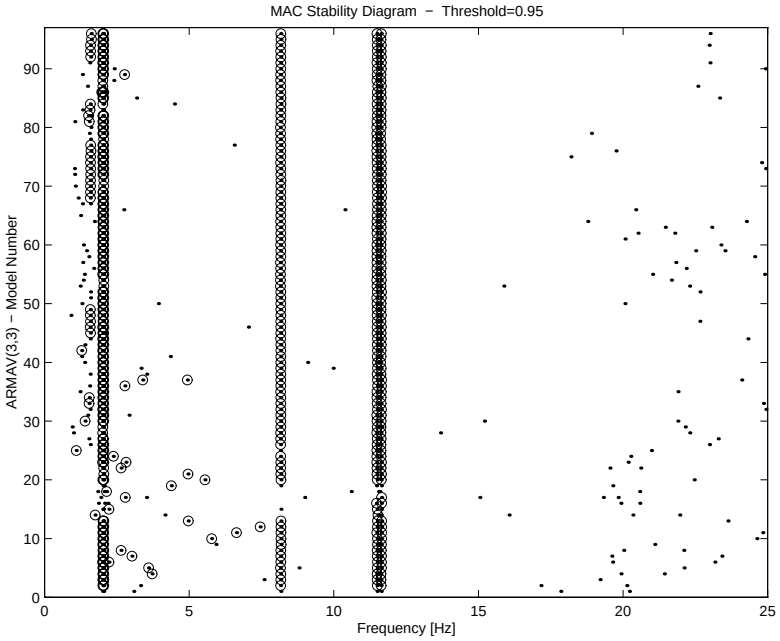

Figure 9.5: MAC stability diagram. A dot "·" indicates an identified mode. If the mode shape of a mode of an estimated model has a MAC value not less than 0.95 with a mode shape of the previously estimated model, then the mode is marked with a circle "o".

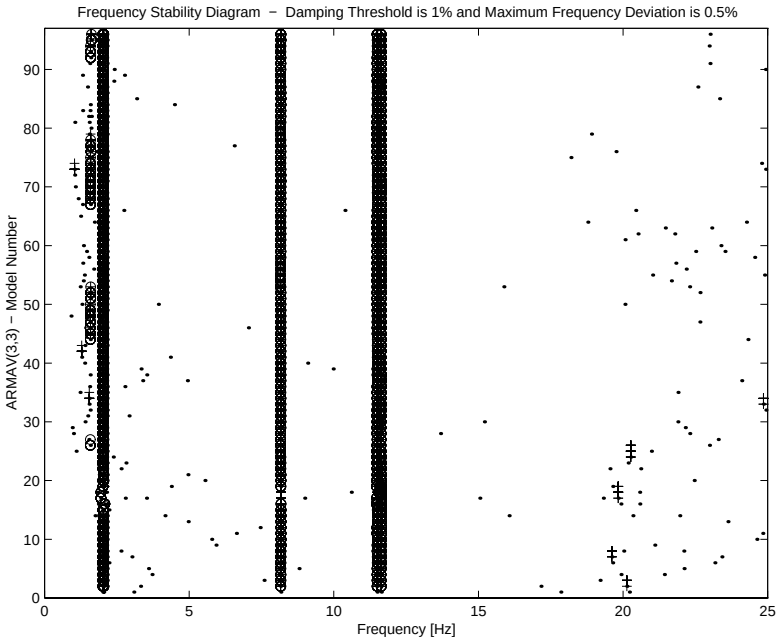

Figure 9.6: Frequency stability diagram. A dot "·" indicates an identified mode. A circle "o" indicates that the damping ratio of the mode is less 1%, whereas a "+" indicates that a particular natural eigenfrequency of a model has been recovered in the previously estimated model with a maximum absolute deviation of 5%.

From the MAC stability diagram, it is seen that two circles are marked around 2 Hz and around 11.5 Hz for almost all estimated models. It is also observed that the modes around 8.1 Hz are marked with a circle. Although it might be difficult to observe, the frequency stability diagram reveals that the two modes around 2 Hz have damping ratios less than 1% for almost all models. This is also observed for the two modes located around 11.5 Hz and the one around 8.1 Hz. Finally, it should be observed that the modes at the same locations are marked with a "+", which indicates that the maximum and absolute deviation of these is less than 5%, between two consequetive model estimates. The average values and sampled standard deviations of all the marked modal parameter estimates of the five structural modes have been calculated. From these values it is also possible to estimate the coefficient of variation, that turns out to be an important parameter in the analysis of the estimated modal parameters in the damaged states. The results are seen in tables 9.1 and 9.2.

Mode #	f_i [Hz]	σ_{f_i} [Hz] $\times 10^{-3}$	$\nu_{f_i} \times 10^{-3}$
1 (Bending)	2.014	2.49	1.24
2 (Bending)	2.044	2.63	1.28
3 (Torsion)	8.166	3.91	0.48
4 (Bending)	11.504	8.66	0.75
5 (Bending)	11.642	5.44	0.46

Table 9.1: Mean values f_i, sampled standard deviations σ_{f_i} and coefficients of variation ν_{f_i} of the natural eigenfrequencies of the five structural modes.

Mode #	ζ_i [%]	σ_{ζ_i} [%]	ν_{ζ_i}
1 (Bending)	0.31	0.14	0.46
2 (Bending)	0.31	0.15	0.48
3 (Torsion)	0.10	0.05	0.48
4 (Bending)	0.18	0.20	1.07
5 (Bending)	0.13	0.06	0.45

Table 9.2: Mean values ζ_i, sampled standard deviations σ_{ζ_i} and coefficients of variation ν_{ζ_i} of the natural eigenfrequencies of the five structural modes.

As seen the coefficients of variation of the estimated natural eigenfrequencies are very small compared to the coefficients of variation of the estimated damping ratios. Since the coefficients of variation of the estimated damping ratios have values between 0.45 and 1.07, it implies that the estimates are very poor. It is therefore not worthwhile to use these estimates in a VBI.

So in conclusion :

☞ *The natural eigenfrequency estimates of the virgin state of five structural modes are very accurately estimated and can thus be used in a VBI if they are unbiased and sensitive to the actual damage.*

On the basis of the results of the previous chapter, concerning the relation between record length and bias, it will be assumed that the estimated natural eigenfrequencies are unbiased.

9.3 Damaged States Analysis

The location of the introduced crack was described in section 1.4.2. In this section, the influence of this growing crack is described. The accuracy of the natural eigenfrequency estimates will be compared with the accuracy of the natural eigenfrequency estimates of the virgin state, and it will be determined which of the natural eigenfrequencies are sensitive to the introduced crack. Finally, a simple damage detection will be performed.

9.3.1 Accuracy Check of Estimated Eigenfrequencies

It is assumed that the structure shows linear and time-invariant behaviour in each damage state. This is a resonable assumption since the size of the crack is extended between the last and the first measurement session of two consequetive damage states. If the size of the crack was increased significantly during a measurement session the system would perhaps behave time-variant. In such a case, it would be necessary to apply an on-line system identification approach. The result of the virgin state analysis was an accurate determination of the natural eigenfrequencies of the five structural modes. From table 9.1, it is seen that the estimation inaccuracies result in coefficients of variation around 1.0×10^{-3}. As described in section 9.2.1, any model that does not have prediction errors that with a resonable confidence form a Gaussian white noise will be rejected. But in addition, natural eigenfrequency estimates with estimated coefficients of variation larger than 1.0×10^{-3} will result in a rejection of the model. In this way the uncertainties of the natural eigenfrequency estimates of the damaged states will qualitatively correspond to the estimates of the virgin state.

9.3.2 Determination of Sensitive Eigenfrequencies

At the present state, it has been established that the natural eigenfrequencies of the five structural modes can be estimated with a high degree of accuracy. However, this does not mean that they can be used as damage indicators. They might simply not be sensitive to the damage. The easiest way to determine whether they are suitable as damage indicators or not is by plotting the estimated natural eigenfrequencies that have passed the rejection criteria described in the previous section.

In the following five figures these estimates will be plotted together with their estimated 95% confidence limits. The confidence limits are determined as $\pm 2\hat{\sigma}_{f_i}$, where $\hat{\sigma}_{f_i}$ is the standard deviation estimated using the technique described in section 6.2.1. The damage state that corresponds to the individual estimate is indicated in the lower plot.

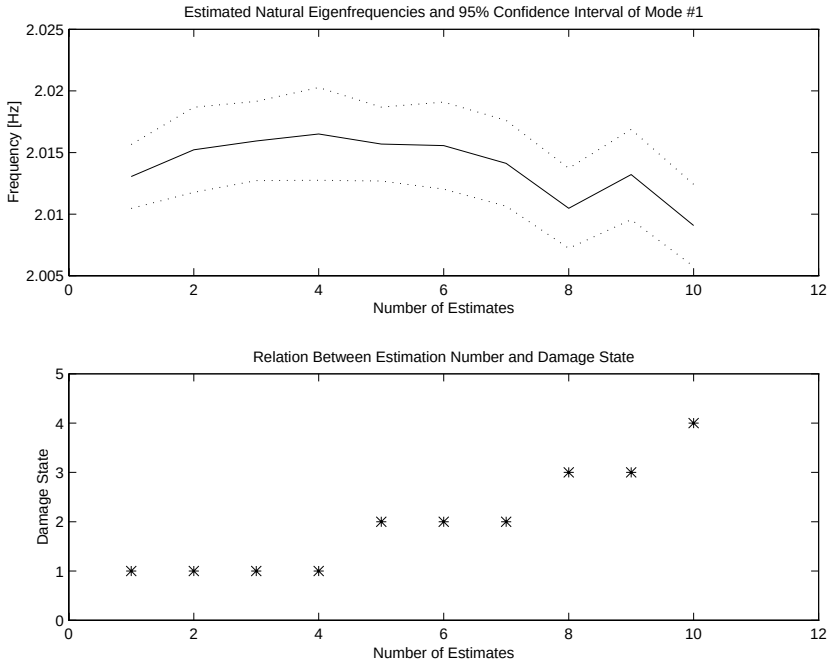

Figure 9.7: Estimated natural eigenfrequencies of the first mode that have passed the rejection criteria. The estimates are plotted together with their estimated 95% confidence interval. The relation between the estimates and the damage states is plotted below.

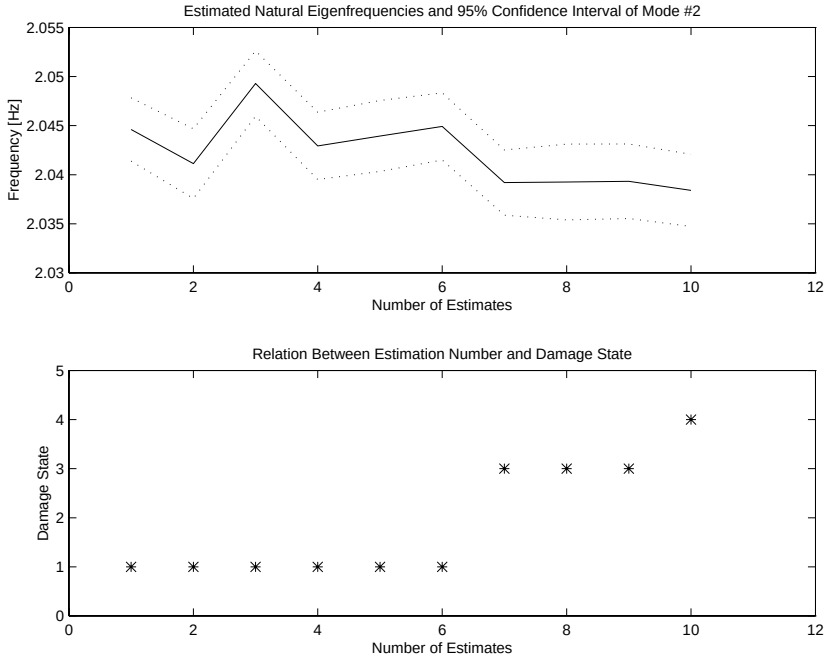

Figure 9.8: Estimated natural eigenfrequencies of the second mode that have passed the rejection criteria. The estimates are plotted together with their estimated 95% confidence interval. The relation between the estimates and the damage states is plotted below.

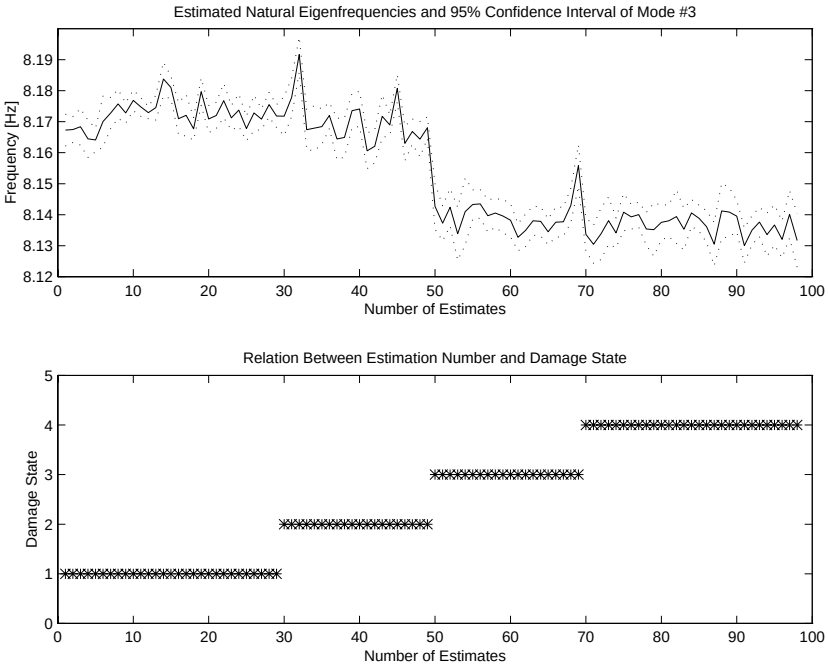

Figure 9.9: Estimated natural eigenfrequencies of the third mode that have passed the rejection criteria. The estimates are plotted together with their estimated 95% confidence interval. The relation between the estimates and the damage states is plotted below.

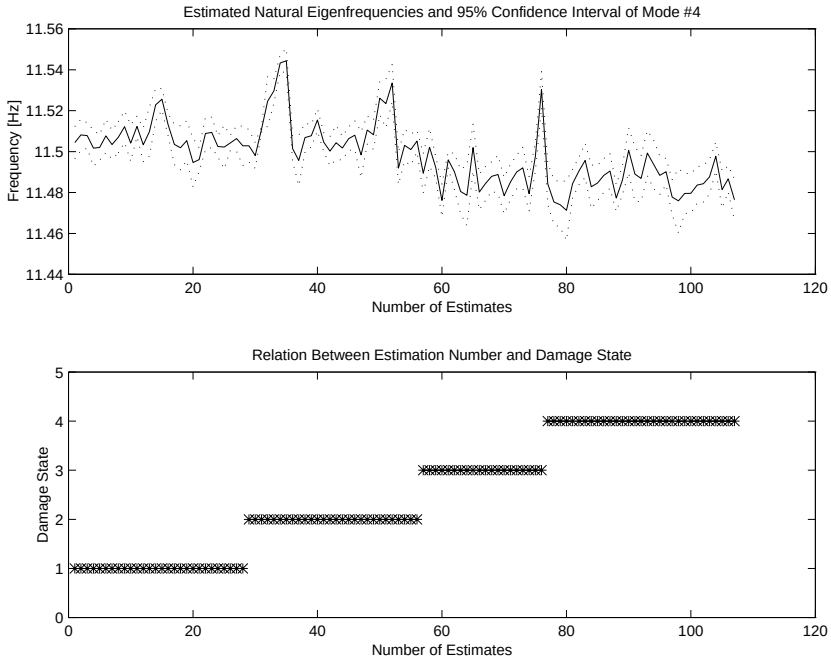

Figure 9.10: Estimated natural eigenfrequencies of the fourth mode that have passed the rejection criteria. The estimates are plotted together with their estimated 95% confidence interval. The relation between the estimates and the damage states is plotted below.

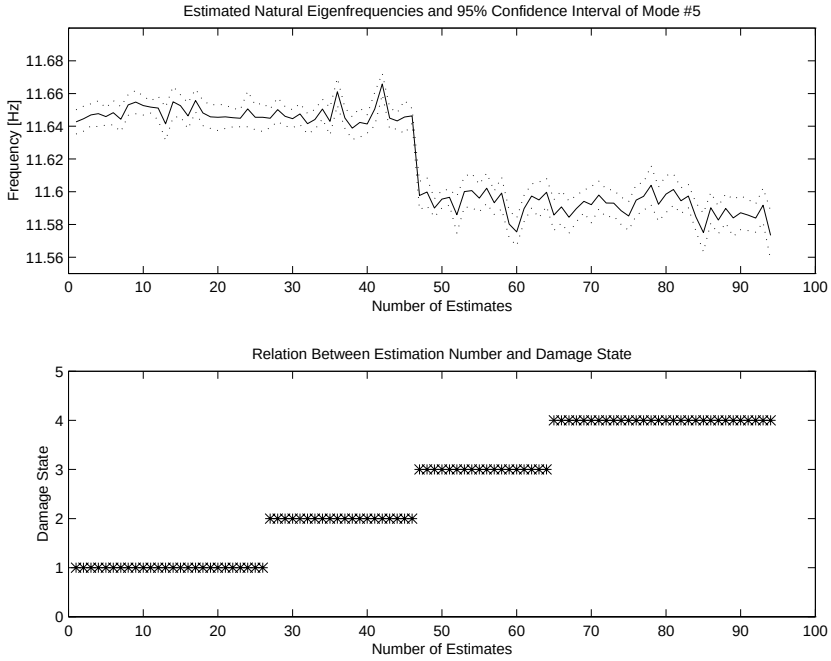

Figure 9.11: Estimated natural eigenfrequencies of the fifth mode that have passed the rejection criteria. The estimates are plotted together with their estimated 95% confidence interval. The relation between the estimates and the damage states is plotted below.

From the five figures, it is seen that the third and fifth mode changes significantly. The changes especially occur when the third damage state is entered. It is seen that in both cases the change from the first to the fourth damage state is so significant that the 95% confidence intervals are seen to be non-overlapping.

So in conclusion :

☞ *It can be concluded that the third and fifth natural eigen-frequency have changed significantly when the final damage state is reached.*

The detected changes of the natural eigenfrequencies are so significant that they probably are caused by a structural change. However, the modal parameters can also exhibit small changes due to fluctuations in the ambient environment. When e.g. the ambient temperature changes, thermal expansion effects and changes of the stiffness will occur. However, it is beyond the scope of this experimental case to consider this influence.

In the context of influence of the ambient environment the effects of fluctuating ambient temperatures on this particular mast have been investigated in Kirkegaard et al. [58], and a technique based on Kalman filtering for removal of such an influence has been proposed in Andersen et al. [7].

9.4 Damage Detection

The above observations imply that the the third and fifth natural eigenfrequencies can be used as damage indicators for this particular damage. The question is at what damage state it is possible to detect the damage with a significant confidence. It will in the following be assumed that a damage has been detected if the confidence intervals of all the natural eigenfrequency estimates of a mode at some damage state are non-overlapping with the 95% confidence interval of the natural eigenfrequency of the same mode in the virgin state. This detection approach can be utilized by plotting the estimates of the third and fifth natural eigenfrequencies and their estimated 95% confidence intervals of the damage states together with the averaged natural eigenfrequency estimates and the estimated confidence intervals of the virgin state. In figure 9.12, this is done for the third natural eigenfrequency estimates, and in figure 9.13 for the fifth natural eigenfrequency estimates.

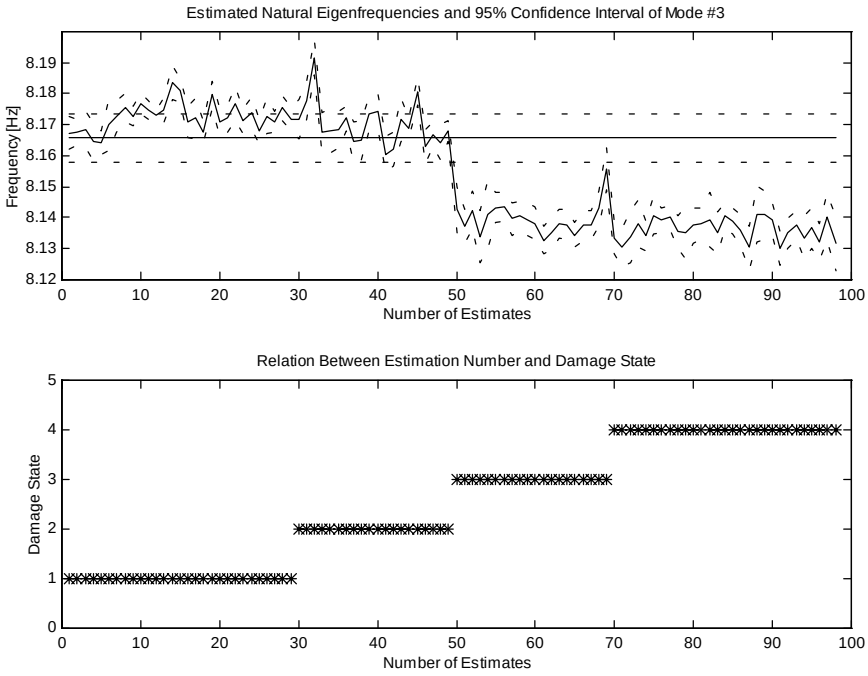

Figure 9.12: Estimated natural eigenfrequencies of the third mode and their estimated 95% confidence intervals.

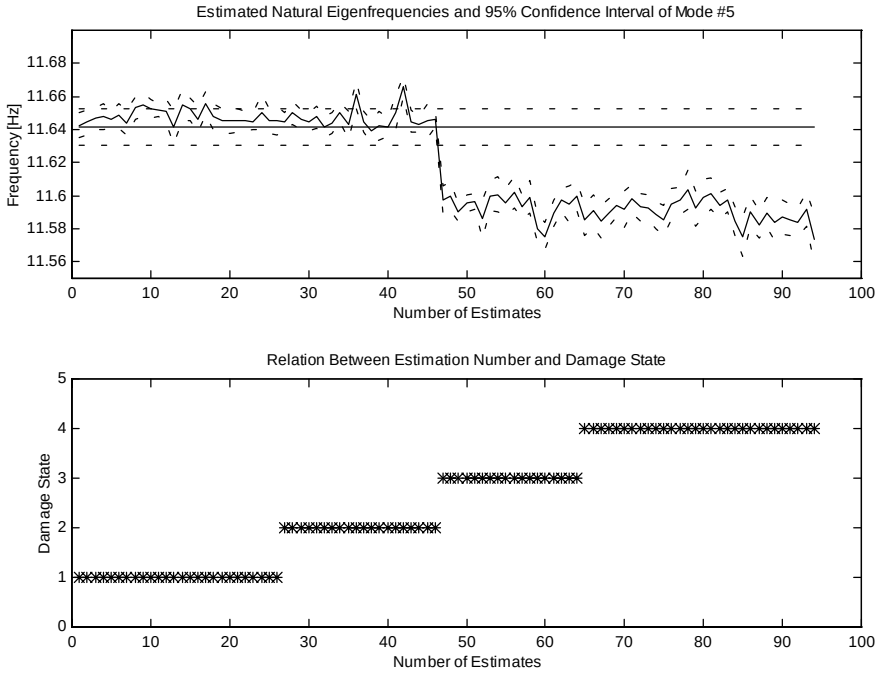

Figure 9.13: Estimated natural eigenfrequencies of the fifth mode and their estimated 95% confidence intervals.

In figure 9.12, it is seen that the confidence intervals become non-overlapping at the moment damage state four is entered. However, already at damage state three the confidence intervals of the natural eigenfrequency estimates of the fifth mode are completely non-overlapping with the virgin state confidence interval, see figure 9.13.

So in conclusion :

☞ *Due to the above definition of a significant damage, it can be concluded that the actual damage has been detected when it entered the third damage state.*

By using the estimated standard deviations, it is actually possible to detect a damage and provide a probabilistic measure of the confidence that should be put in the detection.

9.5 Summary

This chapter has concerned how system identification using ARMAV models can be used in applications such as VBI as a basis for damage detection. By using the ARMAV models accurate natural eigenfrequency estimates have been obtained and their uncertainties have been estimated. Due to the accuracy of the ARMAV estimates, it has been possible to identify two sets of closely spaced modes and to detect significant changes of some of the estimates due to an introduced damage down to a few per cent. By using the estimated standard deviations, the confidence in the significance of these changes has been estimated in a probabilistic sense. The conclusion is that the damage can be detected with a 95% confidence when it enters its third state.